ORIGINAL PAPER

Tilt mapping for zigzag-shaped concrete panel in retaining structure using terrestrial laser scanning

Hyungjoon Seo[1]

Abstract

Traditional monitoring systems are not able to monitor the global behavior of large retaining structures, and terrestrial laser scanning was performed for monitoring a retaining structure for this paper. The three-dimensional point cloud was obtained by scanning at seven locations with seven reference targets to cover the retaining structure having 180 m length and 25 m high. To evaluate the long-term behavior of the retaining structure, point clouds obtained by performing eight laser scanning at the same locations over 4 years were compared with each other. In this paper, the tilt mapping method was applied to define the global behavior of the entire retaining structure. The P2P-TA (Plane-to-Plane-Tilt Angle) comparison method was used to calculate the tilt angle by comparing the normal vectors of the planes created by the point clouds, because simple comparison methods are not able to be applied to compare points clouds of zigzag-shaped concrete panels. A laboratory test was conducted to determine the applicability of laser scanning and P2P-TA analysis, and the error range was conservatively set to 0.15°. The results of laser scanning and P2P-TA analysis applied to 231 concrete panels are shown in the tilt mapping of the retaining structure. The differential tilt angle was significantly increased every year at the bottom of the concrete panel adjacent to the tunnel. It can be seen that the concrete panel having a large differential tilt angle affects the differential tilt angles of others, because it is linked to other concrete panels.

Keywords Retaining structure · Point cloud · Terrestrial laser scanning · P2P-TA comparison method

1 Introduction

A retaining structure is constructed to minimize displacement during the excavation, and various reinforcing materials such as soil nailing and anchor are used for the stability of the structure Seo et al. [29, 30, 32, 34]. To prevent the failure of retaining structure, a study has been conducted to reinforce using pressurized grouting [31]. Seo et al. [33] proposed a reinforcement method in which anchor and soil nailing are combined. To measure the stability, strain gauges are installed in the anchor and the soil nailing, or a sensor is attached to the surface of the structure to evaluate the stability of the structure. Qu et al. used sensors attached to various structures such as bridges or superstructures to determine the stability [19–22]. The eigensystem realization algorithm was used to improve the method of analyzing signals from

various sensors of the sensor [23], Qu et al. [19–22], and also identified closely spaced modes through modified frequency domain decomposition Qu et al. [19, 22]. Contact sensors are difficult to apply to large-scale structures, because only the deformation at the points where sensors are installed can be measured. Therefore, laser scanning technology was applied to collect the three-dimensional data of retaining structure in this paper. Laser scanning can represent not only local curvature and roughness, but also the behavior of global structures as a three-dimensional point cloud [27, 28].

In recent years, three-dimensional (3D) laser scanning has been increasingly applied as a surveying technique, which can scan a wider area using millions of points than conventional surveying techniques. In the geological field, 3D laser scanning is used to prevent natural disasters or to acquire geological geometry. Lague et al. [13] studied the complex ground of Rangitikei canyon by terrestrial laser scanning. 3D laser scanning was applied as a technique for monitoring the displacement of landslides as well. Derron and Jaboyedoff [5] conducted landslide monitoring using LIDAR (Light Detection and Ranging) and DEM (Digital

✉ Hyungjoon Seo
  Hyungjoon.Seo@liverpool.ac.uk

1 Department of Civil Engineering and Industrial Design,
   University of Liverpool, Liverpool L69 3BX, UK

elevation Model) technologies. Girardeau-Montaut et al. [9] used laser scanning to evaluate the ground changes. Since 3D laser scanning technology can simulate objects as a 3D point cloud, it is also used in construction management fields for obtaining geometry data, such as building information modeling (BIM). Gikas [8] also documented the shape of structures using 3D laser scanning at the highway tunnel construction site. 3D laser scanning has the advantage of being able to create 3D shapes in a wide area or a large-scale structure by a point cloud.

Laser scanning techniques have been used as monitoring techniques as well as acquiring three-dimensional geometry. Recently, 3D laser scanning is rapidly developing as a monitoring technique for assessing the stability of various infrastructures. Armesto et al. [4] modeled the masonry arches shape with a terrestrial laser scanning technique, and Riveiro et al. [24] conducted a study to automatically process large point clouds after performing a laser scan through a masonry arch in a bridge. Studies on the settlement and deformation of bridges using point clouds have also been conducted Acikgoz et al. [1], Ye et al. [38]. Soni et al. [35] performed laser scanning for the rail with the conventional surveying techniques. Monitoring of the dam is also a challenge as a huge structure, and González-Aguilera et al. [10] conducted a study to structure monitor of the dam using 3D laser scanning. Fekete et al. [6] applied 3D laser scanning to drill and blast tunnels. Fekete and Diederichs [7] used 3D laser scanning with discontinuum modeling to analyze the stability of the tunnel in blocky rockmasses. Han et al. [11] and Wang et al. [37] conducted a study to measure the deformation of a tunnel through multi-epoch dispersed 3D LIDAR point clouds. Seo [26] applied the 3D laser scanning and distributed fibre optic sensing together for the pile test.

Laser scanning is a non-contact monitoring technique that has been often used to monitor historic buildings without any installation of other sensors, as have 3D cameras and infrared cameras [29]. Schueremans and Genechten [25] used 3D laser scanning to determine the stability of the masonry vaults of the Saint Jacobs church. Armesto-González et al. [3] conducted a study that applied terrestrial scanning to detect damage to historic buildings. Pesci et al. [18] began to study deformation patterns by applying laser scanning to ancient buildings. 3D laser scanning has the advantage of being able to perform non-contact monitoring of the deformation of the structure.

In this paper, a retaining structure was monitored by terrestrial laser scanning. The laser scanning monitoring has been applied to the retaining wall as well and Oskouie et al. [17] conducted a study that applied terrestrial laser scanning to a retaining structure on a highway. Seo et al. [29, 30, 34] conducted monitoring of the concrete panel in the retaining structure. The displacement analysis using point cloud data of a retaining structure was conducted, as well

Seo [27, 28]. Since the results of the laser scanning system are affected by the density of the point cloud, Lin et al. [15] also applied the terrestrial laser scanning having a high resolution to monitor the behavior of mechanically stabilized earth walls with precast concrete panels. Aldosari et al. [2] monitored the concrete panels of the retaining walls with a mobile LiDAR, because a single scan is not able to cover the large-scale retaining structure. In this paper, to obtain the high resolution and the high accuracy, multiple monitoring was performed in various locations. In addition, if the previous studies focused on damage detection, this paper focused on analyzing the variation of the deformation in the retaining structure over time.

To evaluate the deformation of structures, appropriate analysis for point cloud comparison should be applied according to the shape and texture of the structure. The results by applying an appropriate point cloud comparison method can compensate for the low accuracy and low resolution of laser scanning, as well. Lague et al. [13] proposed DEM of difference (DoD), direct cloud-to-cloud comparison with closest point technique (C2C), and cloud-to-mesh distance or cloud-to-model distance (C2M). Girardeau-Montaut et al. [9], and Hodge [12] studied that high roughness surfaces generate occlusion patterns that depend on the viewpoint and introduce complexity in the point cloud comparison. Mitra and Nguyen [16], and Lalonde et al. [14] studied the calculation and orientation of surface normals. The concrete panel scanned in this paper has a rough texture and zigzag shape, so that it is difficult to apply the existing point cloud comparison methods. Therefore, in this paper, the P2P-TA (Plane-to-Plane-Tilt Angle) comparison method was proposed and applied to all concrete panels in the retaining structure using the tilt mapping to determine the stability of the retaining structure globally.

2 Terrestrial laser scanning technology

The terrestrial laser scanner is surveying instruments that use a laser distance meter combined with a rotating mirror. As the unit rotates about a vertical axis on its tripod, a 45° mirror rotates about a horizontal axis. This allows the scanner to measure distances in any direction within a wide field of view. Optionally, a camera within the unit may also be used to provide color information for each measured point. By performing a scan over the entire field of view, the scanner is able to measure millions of separate points in 3D space creating a 3D 'point cloud'. This point cloud may be viewed and manipulated on a computer, and may be viewed from any locations, not just the position from which the scan was originally taken. Typically several scans are taken on the same site from different locations. It can minimize the effect of shadowing; where objects that were obscured from

the view of the scanner would otherwise be absent from the point cloud. During off-site processing of the data, multiple point clouds from different scans can be referenced together to provide a larger, more complete 3D representation.

In this paper, laser scanning was performed to identify the behavior of the retaining structure for a long term. The laser scanner can shoot the laser and collect the reflected laser. A camera can also be installed in the laser scanner to take an overall picture of the site. After the installation of the laser scanner on a tripod, the tribrach and level can be used for leveling the laser scanner (see Fig. 1). In this paper, scanning was performed with a TOPCON gls 2000 scanner [36]. The setting of the interval between points during scanning was 6.3 mm at the distance of 10 m between the scanner and the object. Detailed parameters of the laser scanning system are shown in Table 1.

Laser scanning technology has been used in various fields such as BIM (Building Information Model), because it can represent the shape of the object using a three-dimensional point cloud. The laser scanner shoots millions of laser light toward the object and collects laser points reflected from the object to form a single point cloud (see Fig. 2a). The laser scanner can rotate 360° vertically and horizontally to perform the global scanning for the entire region of object, as well as local scanning can be done after setting a specific scanning area. The distance between the laser scanner and the object can be estimated from the speed of the laser and the time the laser is reflected off the object. Each point in the point cloud can be represented in the X, Y, and Z coordinates of the three-dimensional space using the estimated distance and the vertical and horizontal angles of the scanner. The resolution of the point cloud representing the interval between the laser points can be determined by the distance between the object and the laser scanner. Therefore, if the measurement distance of the laser scanner is too far, it is not able to expect to obtain the higher resolution.

If the object is blocked from other objects from the laser scanner or there are some shadowed areas in the object, the shape of the object is not able to be obtained based on a single scan. Reference targets (checkerboards or magnetically mounted spheres) are positioned around the perimeter of the area to be scanned. These targets are to aid later post-processing of the scan data by allowing two or more scans, which initially have different coordinate systems, to be easily referenced to one another. Point clouds produced by different scans need at least two targets in common to be cross-referenced. The site needs to be assessed to be scanned and to plan a series of locations from which to perform scans such that overlapping scans can minimize the areas of the site that are obscured or 'shadowed', while ensuring that at least three reference targets are in view and in common with neighboring scans. On large sites, it is necessary to move targets used in earlier scans once they are no longer in the view provided three common targets remain between successive scans.

Laser scanning of large-scale infrastructures, such as the retaining structure scanned in this paper, can collect a three-dimensional point cloud of the entire structure by multiple laser scans. To merge laser scan data taken by different locations into one, the local coordinate system used for each scan can be combined into one integrated coordinate system by connecting the reference targets of different scans (registration), as shown in Fig. 2b. In this paper, concrete panels installed as a retaining structure were scanned, which have zigzag-shaped and shadowed areas in concrete panel occur in a single scan, as shown in Fig. 2b. Therefore, at least three locations (Location A, B, and C) are required to remove the shadowed effects in point clouds. In this paper, two or more scans were performed in a location, and the laser scanning of the retaining structure was performed at seven different locations.

As shown in Fig. 2c, different results can be obtained by the position and scanning direction of the scanner. In addition, the density of the point cloud representing the object is varied with the position of the scanner. The point cloud obtained at
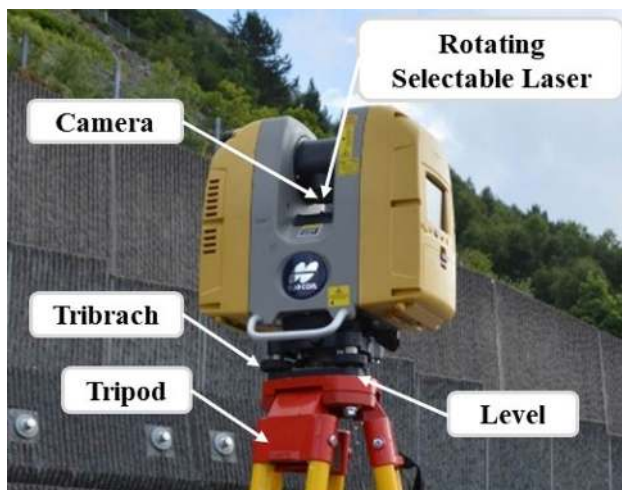

Fig. 1 Laser scanner

Table 1 Parameters of laser scanning

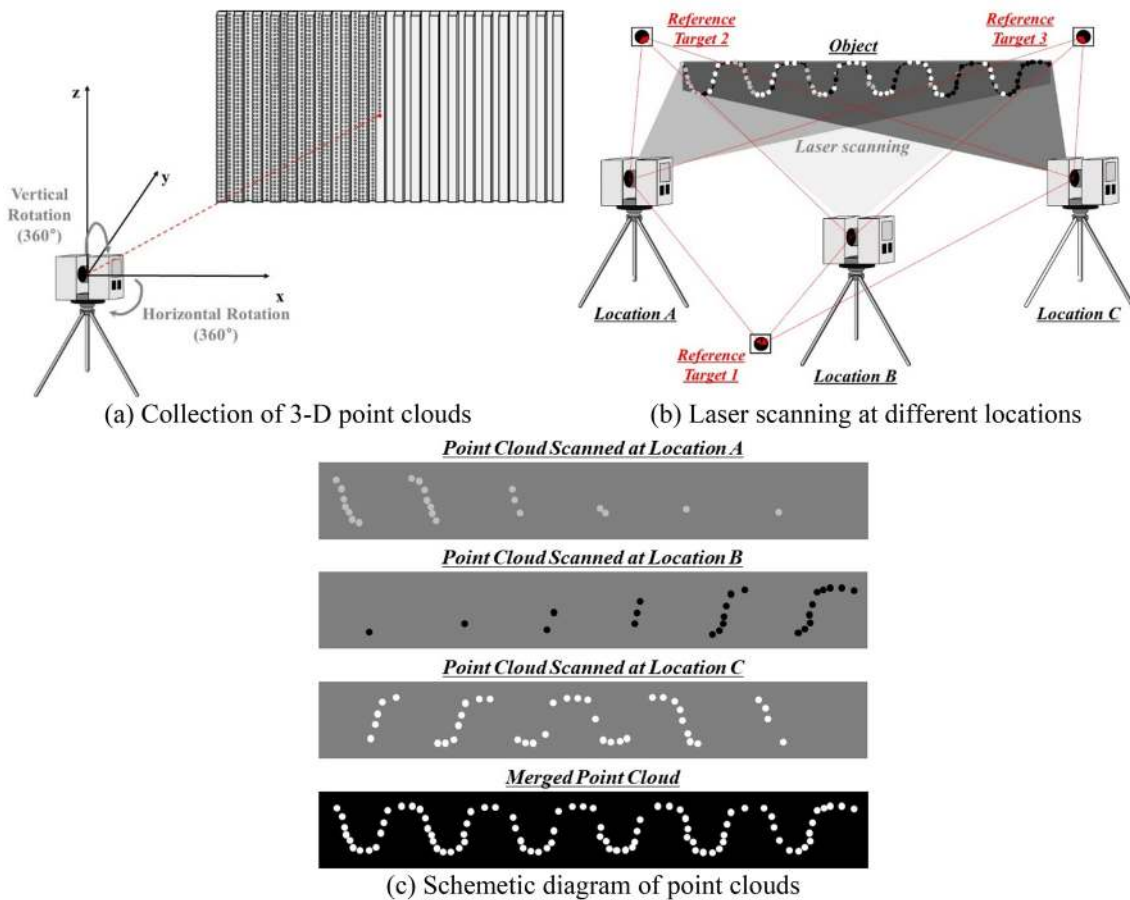| Single point accuracy	Target detection accuracy	Spot size	Operation temperature	Interval in a scan	Operation time
3.5 mm (1—150 m)	3" at 50 m	4 mm at 20 m	− 5 to 45 °C	6.3 mm at 10 m scanning	00:26:44 for a 360° scanning

Fig. 2 Principle of 3D laser scanning

three different locations can be registered in a coordinate system to obtain an integrated point cloud, which can more accurately represent the three-dimensional shape of the structure, unlike the results obtained at each location. In particular, if the surface of the object is severely curved, such as the structure scanned in this paper, it is necessary to secure a plurality of scanning at various locations.

3 Laser scanning in retaining structure and analysis of point cloud

3.1 Introduction of site

A retaining structure located at the tunnel entrance was constructed to facilitate the construction of the tunnel. Anchor bolts were installed into all concrete panels to reinforce the retaining structure. Concrete panel sizes are 4.2 m and 2.0 m, respectively. In the early stages of construction, the strain gauge was installed in the PC strand of the anchor to monitor the stability of the structure continuously, but all strain gauges were damaged due to electromagnetic

problems. As shown in Fig. 3, the retaining structure is about 200 m in length and 25 m in height, and the conventional monitoring system is not able to monitor the global behavior of the entire retaining structure. Although laser scanning technology can be less accurate than conventional monitoring systems, it can cover a wide range of areas in three dimensions. Laser scanning technology is also able to monitor in the long term, because there is no need to install

Fig. 3 Laser scanning location

any instrument on the structure. Therefore, in this paper, to determine the global behavior of the retaining structure in the long term, laser scanning was performed in March and July 2015, April and June 2016, February and July 2017, and February and July 2018, respectively. The data scanned in March 2015 were set as the baseline to compare with the other seven scanning data to evaluate the behavior of the retaining structure for 4 years. Since the scanning was affected by the vegetation in the summer scanning, the scanning was carried out after the weeding.

It is not able to collect the entire point cloud with a single scan in large infrastructures such as retaining structures. Higher resolution can be obtained in the area where the structure and the laser scanner face each other. However, as the distance between the laser scanner and the structure increases, the resolution is decreased linearly. Therefore, scanning was performed at seven positions to cover the 180 m length retaining structure (see Fig. 4a). There were two scans performed at one location: the global scanning with 360° rotation of the laser scanner; and the local scanning obtained by rotating laser scanner left and right 45°. There are 231 concrete panels in a masonry structure. 14 scans were performed to determine the global behavior of all concrete panels. The level of the laser scanner was less than ± 3 "before scanning and no more than ± 5" after scanning in all scans.

During scanning, an interval was set 6.3 mm at 10 m of distance between the laser scanner and the object. The distance between the scanning locations and the retaining structure is about 20 m, so that the resolution is reduced by two times. However, the resolution is increased about six times, because two scans are performed at one location and a scanned area can be covered by scanning at three locations. Therefore, the resolution of the point cloud-shaped concrete panels is decreased to approximately 2 mm. Seven circular reference targets with a diameter of 150 mm were installed to represent all laser scanning data in the same coordinate.

As shown in Fig. 4b, reference targets were installed at the bottom of the column of the streetlight and traffic sign. Although different point clouds can be merged with at least two reference targets, seven reference targets were installed for minimizing the registration error as well as considering the loss of targets and long-term monitoring, and most reference targets can be scanned at all scanning locations.

3.2 Point cloud comparison methods

In this paper, laser scanning was performed to determine the behavior of anchored concrete panels installed in the retaining structure for a long term. The cloud comparison method can be applied to compare the scanned data at different period times. As shown in Fig. 5a, an anchored concrete panel is a zigzag-shaped structure, which can be overestimated or underestimated the movement of a concrete panel without proper cloud comparison. Three methodologies can be mainly applied to compare different point clouds: (a) Cloud-to-Cloud comparison (C2C); (b) Could-to-Mesh comparison (C2M); and (c) Plane-to-Plane comparison (P2P).

Figure 5b shows a schematic diagram of the C2C comparison of the point cloud scanned before and after the movement of the concrete panel. The C2C comparison can simply calculate the distance between the nearest two points. Therefore, as shown in the enlarged figure (see Fig. 5b), the distance between the points (displacement) can be underestimated, because a point at the protruding edge is not able to find a point at the same position for distance calculation and a nearest point can be selected. C2C comparison is not able to be applied to the zigzag structure scanned in this research. C2C comparison is also strongly influenced by the resolution of the point cloud. If the resolution is low, the points in the point cloud are sparse, and hence, the distance between points can be overestimated when the C2C comparison method is applied. To overcome the shortcomings of the C2C comparison method, a C2M comparison method can
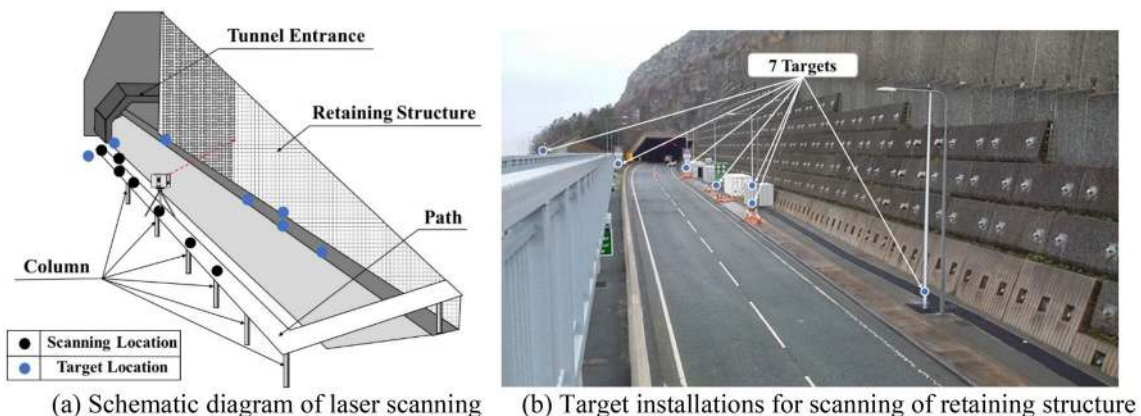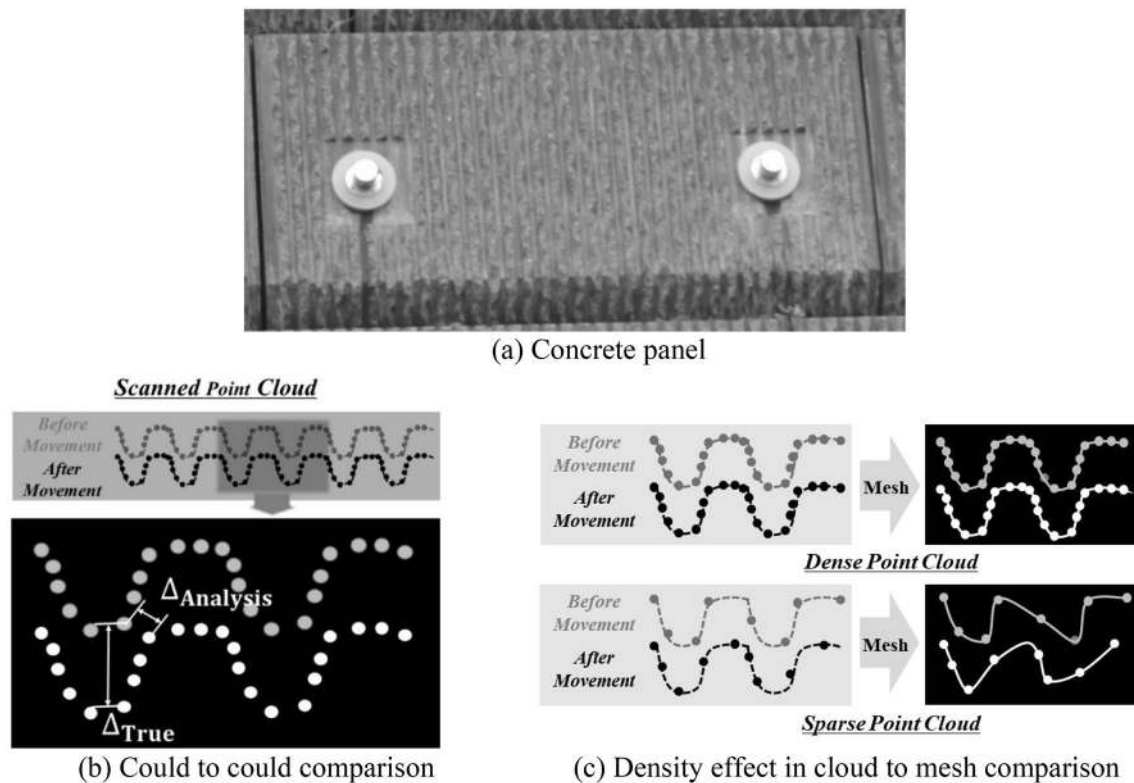

(a) Schematic diagram of laser scanning   (b) Target installations for scanning of retaining structure

Fig. 4 Overview of retaining structure for laser scanning

(a) Concrete panel

Scanned _Point_ Cloud

(b) Could to could comparison

(c) Density effect in cloud to mesh comparison

Fig. 5 Cloud comparison methodologies

be used in which a three-dimensional point cloud is formed into a mesh and then compared between cloud and mesh. Figure 5c shows a schematic diagram of the C2M comparison method. Because C2M comparison compares different point clouds as a mesh, they have more accurate results than C2C comparison, which means that the error caused by the discontinuity between the two points can be minimized. However, the C2M comparison method is heavily influenced by the density of the point cloud. As shown in Fig. 5c, it is possible to create an appropriate mesh that is similar to the actual structure meshing from a dense point cloud, but meshing a sparse point cloud describes an entirely different shape of an actual structure. Therefore, C2M method can produce unexpected results. In this paper, C2C and C2M comparison methods, which can be affected by the particular shape of the structure and resolution of the point cloud, were not applied.

P2P comparison method can be applied to compare point clouds that a point cloud is simulated as a simple plane and then compare the planes. As shown in Fig. 6a, there are four planes included in the zigzag shape of the concrete panel. It can be seen that all four planes lie in the same direction. Therefore, when a plane is created from a point cloud of an entire concrete panel, this plane can have the same directionality as four planes, and hence, it can represent the entire concrete panel. In the P2P comparison method, one plane representing the selected point cloud can be produced, which

means that a plane is selected among lots of planes in three-dimensional space that has the minimum distance between the point cloud and the plane (see Fig. 6b). Planes created by different point clouds are compared as same as C2M comparison method in the P2P comparison. In dense point cloud conditions, the P2P method not only achieves proper results, but also minimizes errors even in sparse point cloud conditions (see Fig. 6c). As shown in Fig. 6a, the four planes are vertically oriented and the vertical rotation of the laser scanner is scanned in the same direction with these planes. In addition, regardless of the density of the point cloud, the laser scanner has the same resolution within a scanned data, so that a plane representing the concrete panel can be obtained from the point cloud even in the sparse point cloud condition. However, since the P2P method obtains only a plane representing an entire concrete panel, the local deformation in the concrete panel is not able to be estimated. The concrete panel has large stiffness, so that this paper focuses on global behavior rather than local deformation within a panel. There are two anchors installed at the center of the concrete panel to reinforce it, and hence, tilt is the main behavior of it. Therefore, this paper proposed is the P2P-TA (Plane-to-Plane-Tilt Angle) comparison method to evaluate the variation of the tilt angles of concrete panels over a long term. As shown in Fig. 6d, the normal vectors are calculated from the planes representing concrete panels before and after
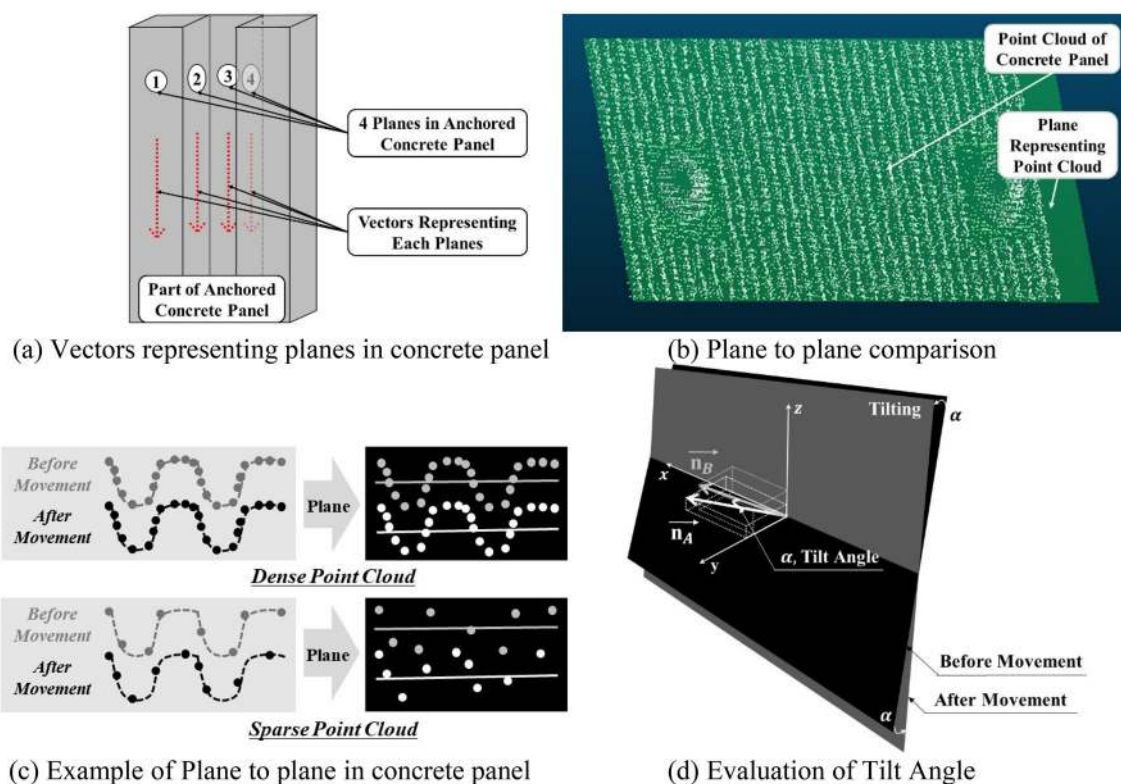
(a) Vectors representing planes in concrete panel

(b) Plane to plane comparison

(c) Example of Plane to plane in concrete panel

(d) Evaluation of Tilt Angle

Fig. 6 P2P comparison method

the movement. The difference between the two normal vectors is equal to the tilt angle (α) between the two planes. In this paper, the P2P-TA comparison method was analyzed for all concrete panels installed in the retaining structure to evaluate the global behavior of the retaining structure.

3.3 Laboratory test for calibration analysis

Factors affecting the accuracy of the laser scanning system should be considered before conducting field experiments. In this paper, because eight scans have been carried out over a long period of time, it is not possible to perform scans at the exact same location. Although there are a number of reference targets, the point cloud data can be affected by the scanning positioning effect, and hence, it has to be identified. The analyzed results of the point cloud are also strongly influenced by the density of the point cloud, as well. Therefore, in this paper, the laboratory model test was conducted to calibrate the effect of these two factors. A zig-zag-shaped wooden panel was made half size of the actual model to simulate the concrete panel (see Fig. 7a). The wooden panel was leaned against the wall and the tilt angle of the wooden panel is increased by inserting a 3 mm-thick plate between the wall and the top of the panel (see Fig. 7b). The tilt angle, which is calculated by the thickness of each plate measured by an electronic caliper before insertion, is used

as a reference to compare with the tilt angle evaluated by the P2P-TA comparison method of point clouds. The terrestrial laser scanning was performed every time five plates were inserted. The laser scanner was re-installed and dismantled repeatedly in the condition that the scanning position is not deviated within 0.5 m of the red dot on the floor, as shown in Fig. 7c, and hence, the positioning effect of the laser scanner is considered. The distance between the laser scanner and the wooden panel was 20 m to simulate under field conditions. To consider the effect of the density of the point cloud, scanning was performed with different setting of intervals as 3.1 mm, 12.5 mm, and 50 mm at 10 m of the distance between the laser scanner and the wooden panel. Three reference targets were installed to register different scanning data at the same coordinates, as shown in Fig. 7d.

It is necessary to confirm the error range to use the P2P-TA comparison method proposed in this paper. If the behavior of the structure occurs within tolerances, calibration analysis is required to verify the reliability of the monitoring system. Figure 8 shows a point cloud obtained from different setting of intervals. The result of scanning at the interval of 3.1 mm at 10 m is shown in Fig. 8a, which shows that the dense point cloud can represent a zigzag shape clearly. In this point cloud, 28,241 points are densely distributed within a circular area with a radius of 0.25 m. However, in the interval of 12.5 mm at 10 m, the points representing the
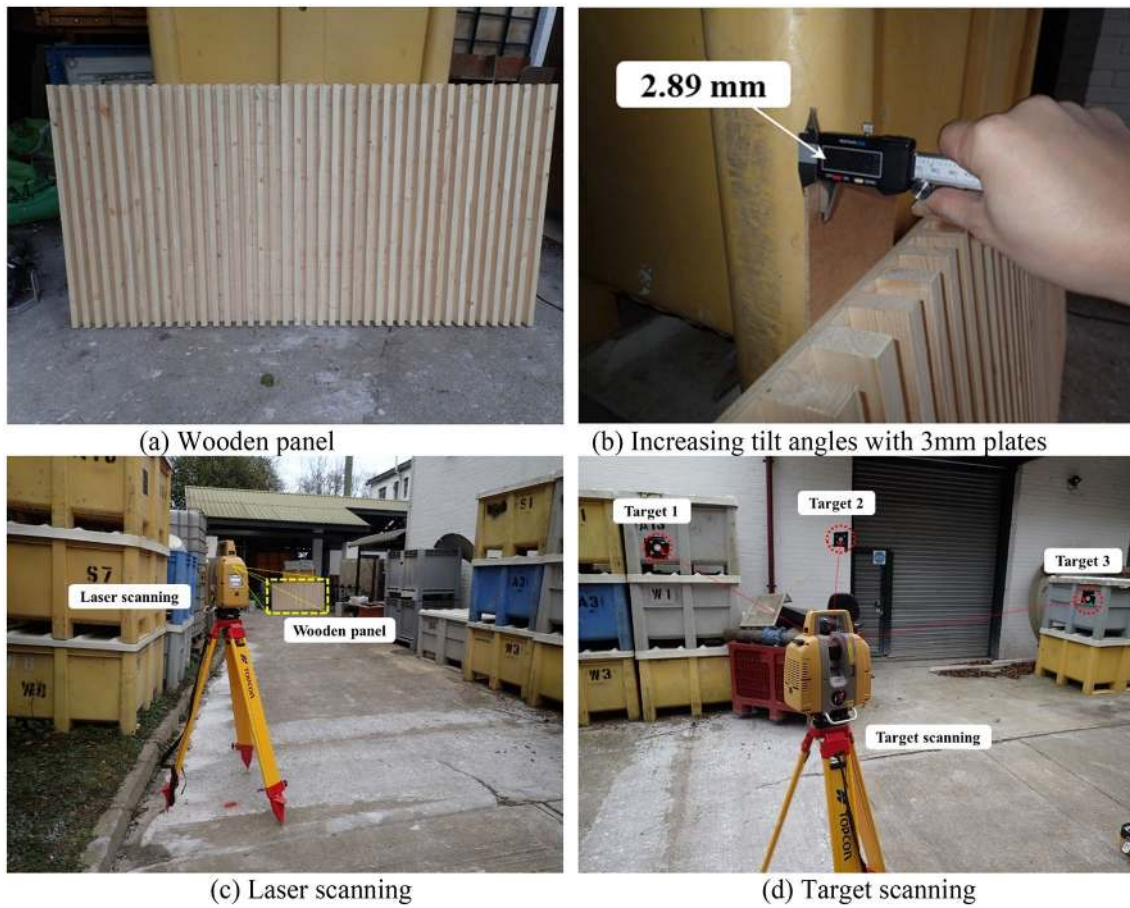
(a) Wooden panel (b) Increasing tilt angles with 3mm plates

(c) Laser scanning (d) Target scanning

Fig. 7 Overview of calibration test

(a) 3.1 mm at 10 m (b) 12.5 mm at 10 m
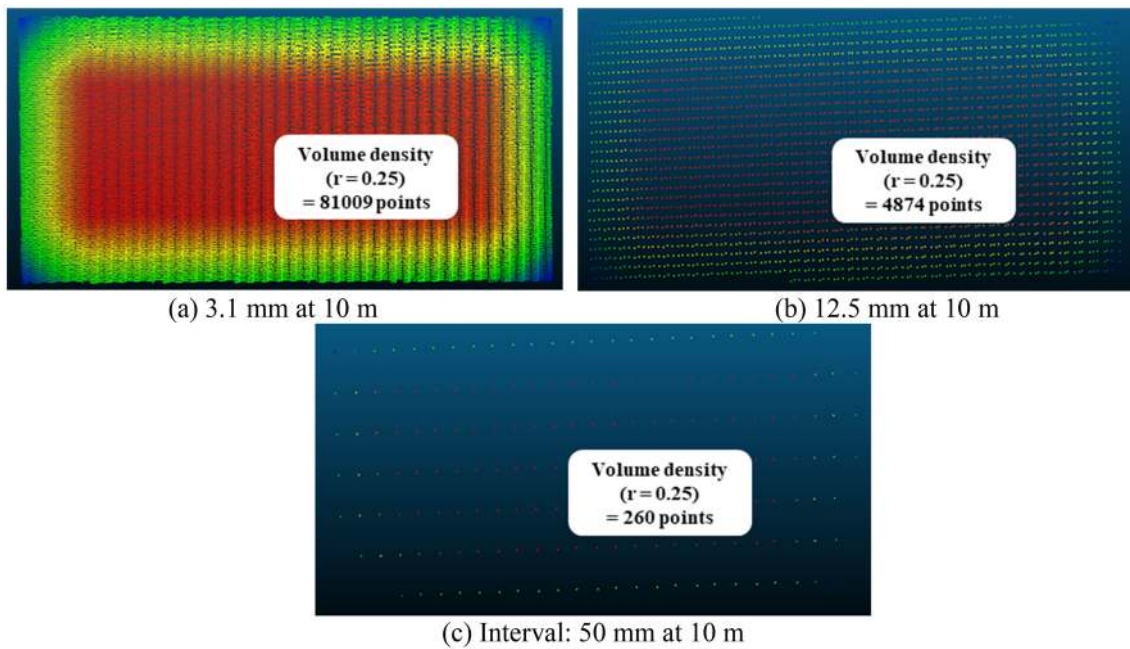
(c) Interval: 50 mm at 10 m

Fig. 8 Density difference in the calibration test

zigzag shape are sparser than that of the interval of 3.1 mm. As shown in Fig. 8b, there are 1763 points within a circular area with a radius of 0.25 m. As shown in Fig. 8c, when the interval is changed to 50 mm at 10 m, the points existing within a circular area with a radius of 0.25 m are significantly decreased to 73, so that the zig-zag shape is not able to be formed. If the spacing between points is sparse, the C2C and C2M comparison methods overestimate or underestimate the distance between two different point clouds, as explained in Fig. 5. In this paper, the calibration analysis is performed to evaluate the applicability of the P2P-TA comparison method analyzing the point cloud data represented with different intervals, as shown in Fig. 8.

The P2P-TA comparison method can calculate the tilt angle from normal vectors of the planes simulated from point clouds. Figure 9a shows the increase of the tilt angle variation evaluated by the P2P-TA comparison method with the increase of the plate number. The differential angles can be estimated by calculating the increase using a point cloud scanned without a plate as a baseline. All results of three cases of intervals show a linear increase. The tilt angles of three cases evaluated by the P2P-TA comparison method are compared with a reference value which is the tilt angle calculated by measuring the plate thickness to determine the error. The results of the interval of 50 mm at 10 m have the largest difference compared to the reference value. The error can be estimated from the difference between the tilt angle calculated by the P2P-TA comparison method and the reference value, as shown in Fig. 9b. In the case of the interval of 50 mm, it can be seen that the maximum error is about 0.27°. However, the maximum error is around 0.04° for the case of the interval of 12.5 mm and around 0.02° for the case of the interval of 3.1 mm. The point clouds obtained from the field test have a higher resolution than those of the interval of 3.1 mm in a laboratory test. However, the factors affecting to generate the error of the result in the laboratory test are better controlled compared to those of the field test. In this paper, 0.15° was set as the maximum error conservatively and applied to field test results.

4 Results of laser scanning for retaining structure

The process of merging point clouds represented on different coordinates into the same coordinate is called registration. There are two registration processes in this paper. The first process is to merge the point clouds scanned at seven locations as one point cloud. Eight scannings were carried out for 4 years, and a set of scanning data includes 14 point clouds from seven scanning locations. Therefore, 14 different point clouds have to be merged into one group. Eight sets of scan data acquired at different time periods are grouped separately to form an individual point cloud. After the first grouping process, eight grouped point clouds obtained at different time points have to be registered in one coordinate system to apply the P2P-TA comparison method. The eight grouped point clouds are superimposed together on the same coordinate. Therefore, all areas representing concrete panels in eight grouped point clouds can be cut together to be compared with each other. After cutting, the P2P-TA comparison method can be applied to evaluate the variation of tilt angles between the baseline and other seven grouped point clouds.

In the registration process, there is a possibility to generate an error caused by the target scanning. In this paper, most registration errors are less than 1 mm or equal to 0. In some scanning cases, the registration error occurred 3–5 mm, but it was removed when the re-registration process was performed without the certain reference targets that caused the large registration error. In this paper, registration error by target scan can be minimized, because seven target scanning were performed. After registration, the density of one
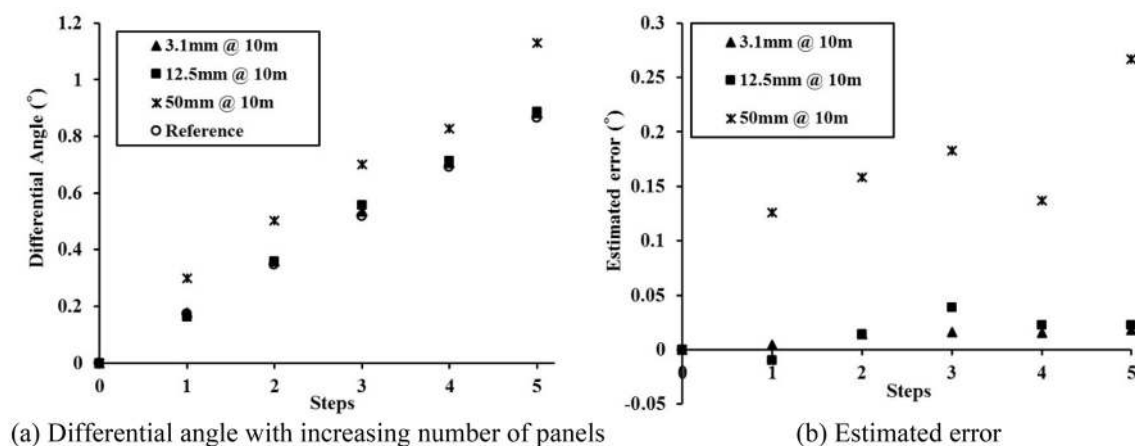

(a) Differential angle with increasing number of panels

(b) Estimated error

Fig. 9 Calibration test in three different intervals

grouped point cloud was checked and it was confirmed that denser points were formed than the density used in the laboratory calibration test. Figure 10a shows an integrated point cloud after completing the registration of all point clouds. The integrated point cloud has obstacles such as vegetation, street lamps, and traffic signs. As shown in Fig. 10b, point clouds after cutting the points representing obstacles can be formed only the retaining structure.

To perform the tilt mapping, 231 concrete panels are segmented from the original point clouds which are arranged in 41 rows and 11 columns in the retaining structure. After registration, eight sets of point clouds can be superimposed together in Cloud Compare software, as shown in Fig. 11, and the point clouds representing the concrete panel can be cut out individually. The point cloud of 231 sets of concrete panels can be extracted from the raw data, and the extracted point clouds are analyzed by P2P-TA comparison method.

In this paper, the boundary of the tilt angle was set by the laboratory model test. However, actual concrete panels have a rougher surface than wooden panels simulated in the laboratory model test. Therefore, it is necessary to identify the dispersion of points with the plane when the plane is shaped in the point cloud representing the concrete panel. If the distance between the points and the plane is irregular, it is not able to apply the P2P-TA comparison method. An area-like plane ① of Fig. 6a was selected, as shown in Fig. 12a. After creating the plane in the selected area, C2M analysis was performed between the plane and the point cloud used to make the plane. Figure 12b shows the dispersion of points within the selected area. The distribution of points with the distance between the points and the plane is shown in Fig. 12c. In all cases where the points are dense, sparse, and intermediate, the trend of points distribution shows a normal distribution, which means that the points forming the plane are not distributed irregularly. For a dense point cloud, the standard deviation of 90% probability is 0.00266 m. 90% of the total points in the selected area are within 0.00266 m between points and plane and 50% of the selected points are within 0.00089 m. In the case of a sparse point cloud, 90% and 50% of the total points are distributed within 0.00230 m and 0.00082 m, respectively, between the point cloud and the plane within the selected area. In the intermediate case, 90% and 50% of the total points are distributed within a distance of 0.00271 m and 0.00098 m. To compare the distribution
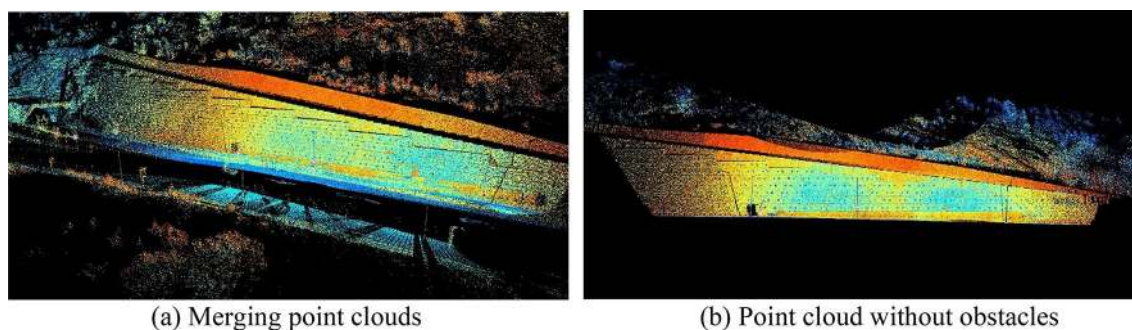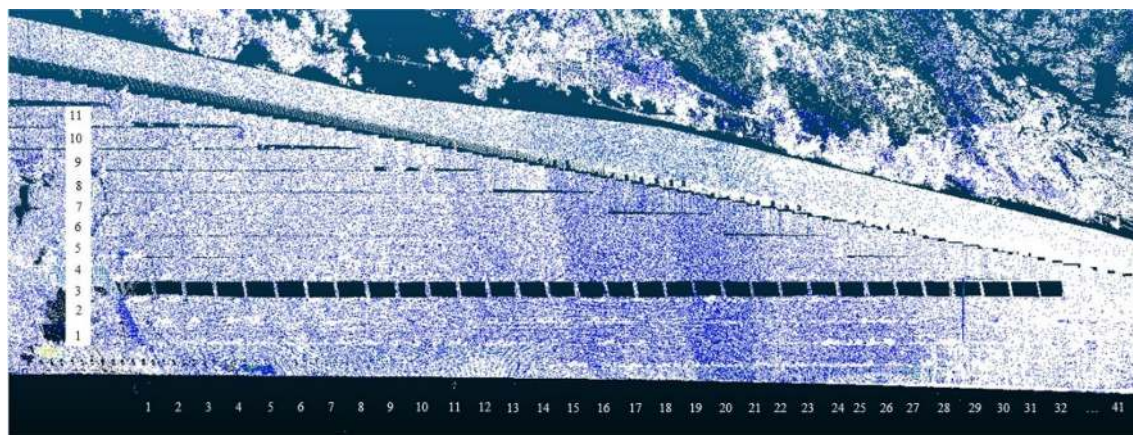

(a) Merging point clouds

(b) Point cloud without obstacles

Fig. 10 Registration of point clouds

Fig. 11 Arrangement of extracted point cloud of concrete panel

(a) Selected area in concrete panel   (b) C2M comparison between selected points and plane

(c) Points distribution with distance   (d) Normalized number of points with distance
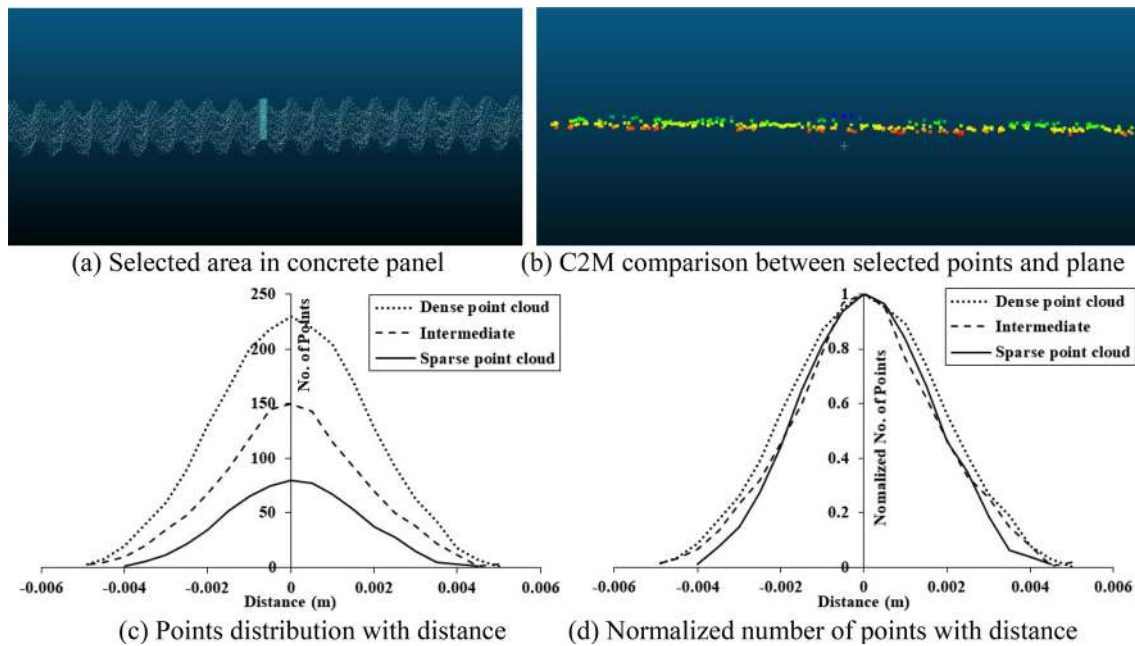
Fig. 12 Dispersion of clouds from plane

trend of the three cases, the number of points was normalized by dividing the number of points by the maximum number of points in each distance (see Fig. 12d). In all three cases, the point cloud densities are different, but the trend of the distributions along the distance between the plane and the points is similar. All three cases have the relation of normal distributions between the plane and the points in the selected area, and the deviations are narrow. Therefore, it can be analyzed by the P2P-TA comparison method as explained in Fig. 6.

The P2P-TA analysis was performed by extracting all 231 point clouds representing concrete panels from the entire point cloud. Since one concrete panel contains eight times scanned data over 4 years, the number of concrete panels is 1848. As shown in Fig. 6d, the differential tilt angle of each panel over 4 years can be evaluated by calculating the difference of the normal vectors of the eight panels from the baseline. Figure 13 shows the tilt mapping of retaining structure composed of concrete panels analyzing eight scans over 4 years. If the differential tilt angle is less than 0.15°, it is within an error range considering the accuracy of the laser scan. When the differential tilt angle is larger than 0.15°, the color representing the panel can be changed depending on the degree of the increase of the tilt angle. The scanned data in July 2015 show that the concrete panels located at the bottom of the retaining structure close to the tunnel are changed in the tilt angle compared to the scanned data in March 2015 (see Fig. 13a). The tilt angle of most concrete panels except this region is smaller than the error range set in this paper, 0.15°. If the location

of the panel is closer to the tunnel, the higher earth pressure applies to the retaining structure due to the increase of the structure height. The bottom of the retaining structure near the tunnel can be applied by the greatest earth pressure, as well. The results obtained in April and June 2016 show that the differential tilt angles of the concrete panels at the bottom of the retaining structure close to the tunnel also are changed (see Fig. 13b, c). In the results of fifth scanning in February 2017, the bottom area near the tunnel which showed the larger variation of the tilt angle is wider than previous results (see Fig. 13d). It can be seen that the differential tilt angles of the concrete panels located at the top of each column are increased, as well. These concrete panels are easy to tilt, because the upper part of the concrete panel is not in a constrained condition. In 2017, there were works such as installing sensors on the panels performed by installing rails on the top of the retaining structure, and hence, it can generate the tilt of the concrete panel. The differential tilt angles are a negative value, because there is no constraint condition at the upper part of the concrete panel. In particular, the results of February and June 2017 show that the differential tilt angle increases in the bottom of the retaining structure and transferred to the horizontal direction (see Fig. 13e). The results of the fifth scanning in February 2018 show that the area where the tilt angle increases are expanded from the bottom panel near the tunnel to others. This trend is also shown in Fig. 13f in the eighth scanning. In particular, it can be seen that the concrete panel located in row 1 and column 3 has a large increase in the tilt angle for 2 years.
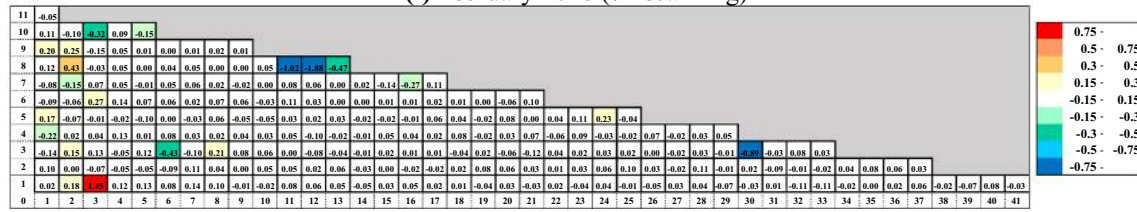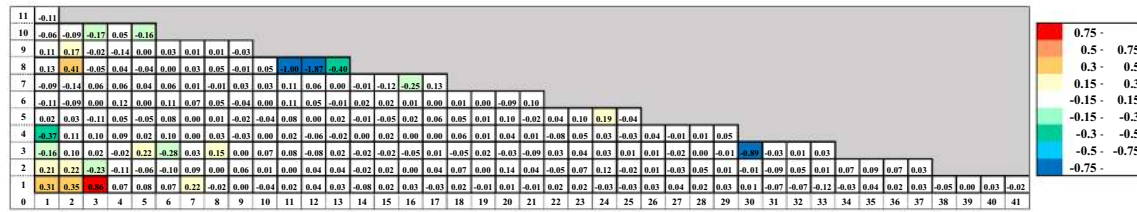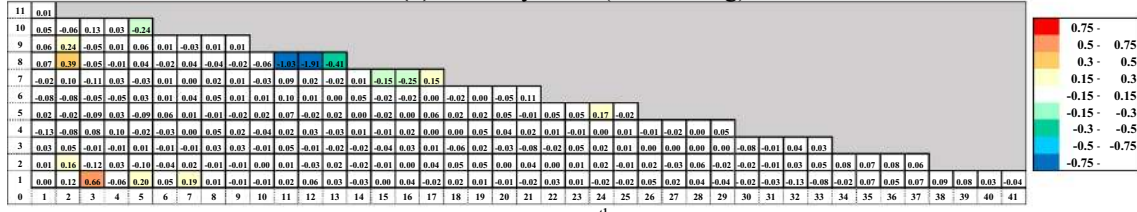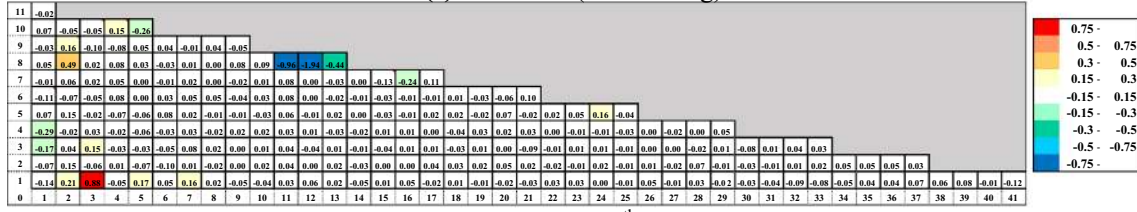
(a) July 2015 (2nd scanning)

(b) April 2016 (3rd scanning)

(c) June 2016 (4th scanning)

(d) February 2017 (5th scanning)

(e) June 2017 (6th scanning)

(f) February 2018 (7th scanning)
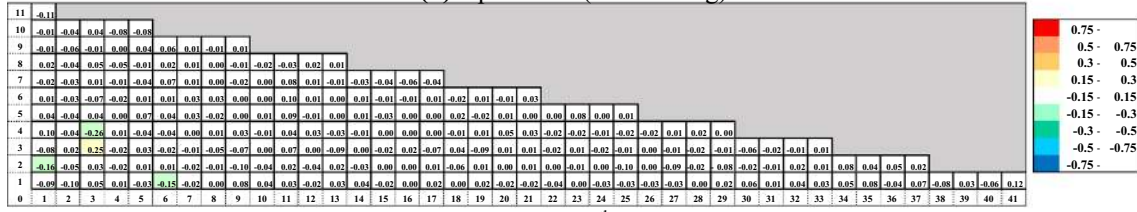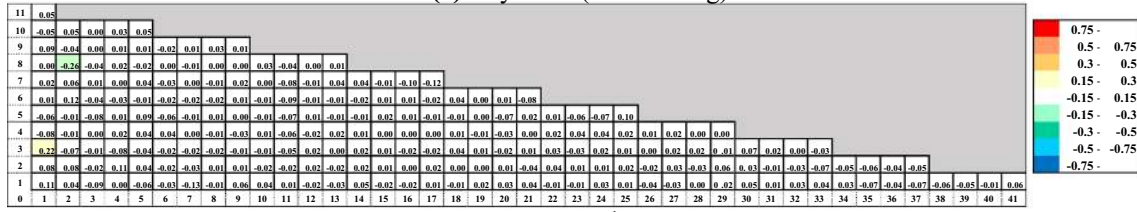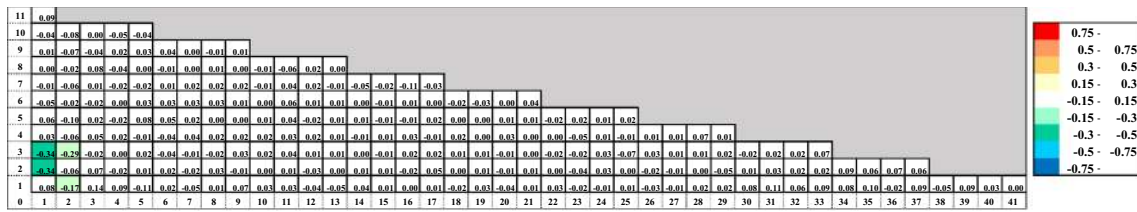
(g) July 2018 (8th scanning)

Fig. 13 Tilt mapping of retaining structure for 4 years

As a result of analysis in Fig. 13, it was confirmed that the differential tilt angle at the bottom of the concrete panels near the tunnel was larger than those in other places. Figure 14 shows the profiles of the differential tilt angle in the horizontal direction of a retaining structure. To estimate the global behavior in each column of the concrete panel, the average value of the absolute differential tilt angle for each column is shown in Fig. 14a. However, the panels located at the highest level of each column were excluded to calculate the average, because those have irregular behavior without constraints. The average value of the differential tilt angle is increased, if panels are located close to the tunnel. It is more intense with the time and within the fifth column of concrete panels. The average value between the fifth and tenth columns is slightly increased due to the increases in the differential tilt angles at some panels located in 1 and 3 rows. From the tenth column onwards, the average values are within the error in every analyzed data regardless of the scanning duration. It was confirmed by the average value of each column that the variation of the tilt angle was prominent at the bottom of the retaining structure near the tunnel. To evaluate the variation of the tilt angle at the bottom of the retaining structure precisely, the profile of differential tilt angles in the first row of the concrete panels is shown in Fig. 14b. In particular, it can be seen that the differential

tilt angle located in row 1 and column 3 is significantly increased after the fifth scanning of the concrete panel. Most of the panels also show positive values after the fifth scanning in the first row. A positive differential tilt angle means that the concrete panel is erected by the horizontal earth pressure at the rear of the retaining structure, which affects the increase of the tilt angle. The differential tilt angle of the concrete panel located in the row 2 and column 3 has a negative value. This is because, as shown in Fig. 14c, the movement of a panel affects the other, because the concrete panels are linked together. When the panel in the row 1 and the column 3 is erected, the panel in the row 2 and the column 3 can be lied down unless there is the horizontal movement with the panel in the row 1 and the column 3. Therefore, the variation of the tilt angle of the panel in row 1 and column 3 affects the other panels in the bottom of the concrete panel near the tunnel. The variation of tilt angle was the largest in the eighth scanning results. Figure 14d shows the average monthly temperature over the 4 years during scanning. In 2018, the temperature change between February and August was particularly larger than in other years. Therefore, it is expected that the concrete panel is much more affected by the thermal expansion.

In this paper, the global behavior of the retaining structure was evaluated by the variation of the tilt angle of the
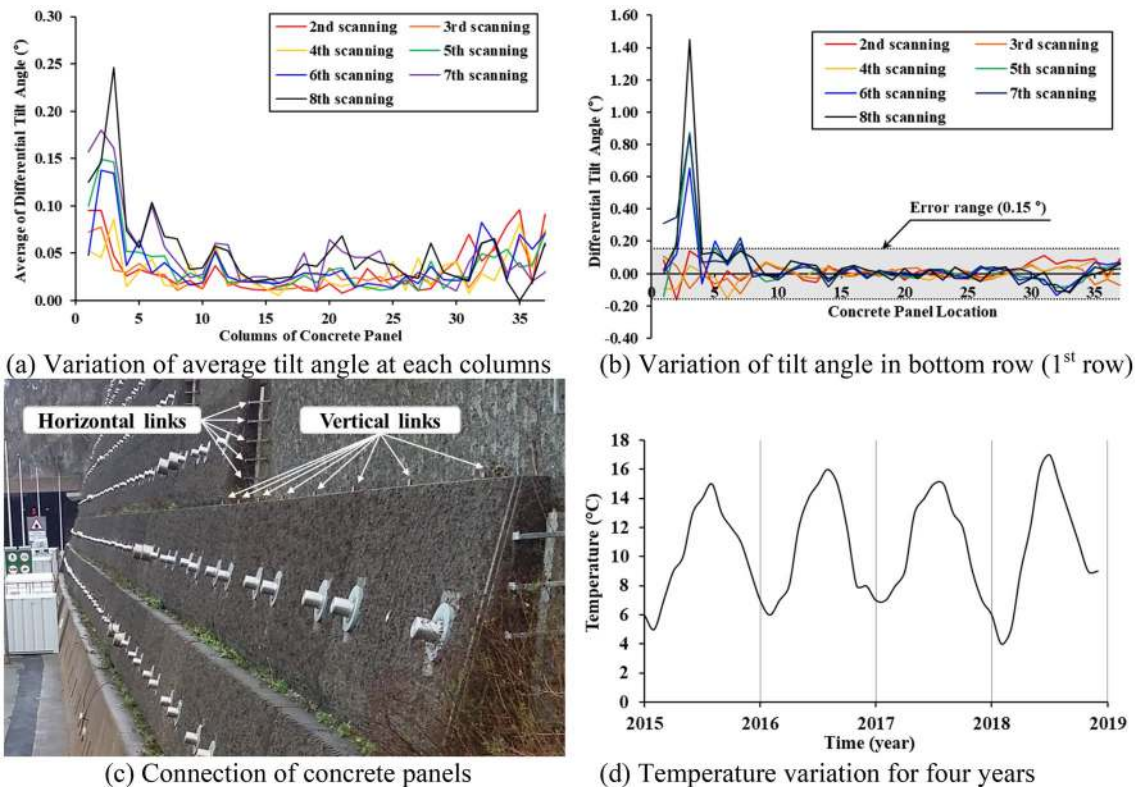

(a) Variation of average tilt angle at each columns

(b) Variation of tilt angle in bottom row (1st row)

(c) Connection of concrete panels

(d) Temperature variation for four years

Fig. 14 Variation of differential tilt angle in the horizontal direction of retaining structure

concrete panel installed with the anchor. Traditional monitoring methods are not able to evaluate the behavior of the entire retaining structure, but the laser scanning method with the P2P-TA comparison method proposed in this paper is able to determine the global behavior of the retaining structure. While laser scanning can monitor large structures in three dimensions, the accuracy of laser scanners is insufficient as a monitoring technique compared to traditional monitoring methods. Therefore, it is more effective to evaluate the global area by laser scanning system and then apply it with the existing high-accuracy monitoring method to local areas that require detailed monitoring.

5 Conclusions

This paper evaluated the global behavior of retaining structure by the P2P-TA comparison method after monitoring the retaining structure composed of anchored concrete panels over 4 years by the terrestrial laser scanning. The results of this study are summarized as follows:

1. The point cloud comparison methods like C2C and C2M cannot be applied to this research due to the zigzag shape of concrete panel. In this paper, the P2P-TA comparison method was proposed that calculates the tilt angle from the normal vector of the plane simulated by a point cloud. The P2P-TA comparison method was applied to 231 concrete panels to determine the behavior of the retaining structure.
2. The error range of the P2P-TA comparison method was estimated as 0.15° in the laboratory calibration test considering the effects of positioning and density of laser scanning. The reason the P2P-TA comparison method can be applied is because all planes in a concrete panel have the same direction vertically. It was proved by analysis of three-point cloud data with different density obtained from the field. Therefore, it was possible to apply laser scanning and P2P-TA comparison methods at this site.
3. The overall behavior of a retaining structure was verified by the tilt mapping method over 4 years, and concrete panels having larger differential tilt angles than the error range were identified. The differential tilt angle at the bottom of the concrete panels near the tunnel was larger than those in other places because of the effect of horizontal earth pressure. Particularly, it was confirmed that a panel in row 1 and column 3 showed the largest change of the tilt angle, and the concrete panels were also linked to each other to affect the other panels.

Laser scanning was able to evaluate the global behavior of the entire retaining structure, but the accuracy was not high enough for detailed analysis. If laser scanning is applied with other monitoring techniques having a higher accuracy, those monitoring systems can complement each other.

References

1. Acikgoz S, Soga K, Woodhams J (2017) Evaluation of the response of a vaulted masonry structure to differential settlements using point cloud data and limit analyses. Constr Build Mater 150:916–931
2. Aldosari M, Al-Rawabdeh A, Bullock D, Habib A (2020) A Mobile LiDAR for Monitoring Mechanically Stabilized Earth Walls with Textured Precast Concrete Panels. Remote Sens 12(2):22. https://doi.org/10.3390/rs12020306
3. Armesto-González J, Riveiro-Rodríguez B, González-Aguilera D, TeresaRivas-Brea M (2010) Terrestrial laser scanning intensity data applied to damage detection for historical buildings. J Archaeol Sci 37(12):3037–3047
4. Armesto J, Roca-Pardiñas J, Lorenzo H, Arias P (2010) Modelling masonry arches shape using terrestrial laser scanning data and nonparametric methods. Eng Struct 32(2):607–615
5. Derron MH, Jaboyedoff M (2010) LIDAR and DEM techniques for landslides monitoring and characterization. Nat Hazard 10:1877–4879
6. Fekete S, Diederichs M, Lato M (2010) Geotechnical and operational applications for 3-dimensional laser scanning in drill and blast tunnels. Tunn Undergr Space Technol 25(5):614–628
7. Fekete S, Diederichs M (2013) Integration of three-dimensional laser scanning with discontinuum modelling for stability analysis of tunnels in blocky rockmasses. Int J Rock Mech Min Sci 57:11–23
8. Gikas V (2012) Three-dimensional laser scanning for geometry documentation and construction management of highway tunnels during excavation. Sensors 12(8):11249–11270
9. Girardeau-Montaut D, Roux M, Marc R, Thibault G (2005) Change detection on points cloud data acquired with a ground laser scanner. Int Arch Photogramm Remote Sens Spatial Inf Sci 36:30–35
10. González-Aguilera D, Gómez-Lahoz J, Sánchez J (2008) A new approach for structural monitoring of large dams with a three-dimensional laser scanner. Sensors 8(9):5866–5883

11. Han JY, Guo J, Jiang YS (2013) Monitoring tunnel deformations by means of multi-epoch dispersed 3D LIDAR point clouds: an improved approach. Tunn Undergr Sp Technol 38:385–389

12. Hodge R (2010) Using simulated Terrestrial Laser Scanning to analyse errors in high-resolution scan data of irregular surfaces. ISPRS J Photogramm Remote Sens 65(2):227–240

13. Lague D, Brodu N, Leroux J (2013) Accurate 3D comparison of complex topography with terrestrial laser scanner: application to the Rangitikei canyon (N-Z). ISPRS J Photogramm Remote Sens 82:10–26

14. Lalonde J-F, Unnikrishnan R, Vandapel N, Hebert M (2005) Scale selection for classification of pointsampled 3D surfaces. In: Proceedings of the fifth International Conference on 3D digital imaging and modeling, pp 285–292

15. Lin YJ, Habib A, Bullock D, Prezzi M (2019) Application of high-resolution terrestrial laser scanning to monitor the performance of mechanically stabilized earth walls with precast concrete panels. J Perform Construct Fac 33(5):04019054

16. Mitra NJ, Nguyen A (2003) Estimating surface normals in noisy point cloud data. In: Proceedings of the Nineteenth Conference on computational geometry, pp 322–328

17. Oskouie P, Becerik-Gerber B, Soibelman L (2016) Automated measurement of highway retaining wall displacements using terrestrial laser scanners. Autom Construct 65:86–101

18. Pesci A, Casula G, Boschi E (2011) Laser scanning the Garisenda and Asinelli towers in Bologna (Italy): detailed deformation patterns of two ancient leaning buildings. J Cult Herit 12(2):117–127

19. Qu C-X, Mei D-P, Yi T-H, Li H-N (2018) Spurious mode distinguish by modal response contribution index in eigensystem realization algorithm. Struct Des Tall Sp Build. https://doi.org/10.1002/tal.1491

20. Qu C-X, Yi T-H, Li H-N (2019) Mode identification by Eigensystem realization algorithm through virtual frequency response function. Struct Control Health Monit. https://doi.org/10.1002/stc.2429

21. Qu C-X, Yi T-H, Li H-N (2019) Modal identification for superstructure using virtual impulse response. Adv Struct Engg. https://doi.org/10.1177/1369433219862951

22. Qu C-X, Yi T-H, Li H-N, Chen B (2018) Closely spaced modes identification through modified frequency domain decomposition. J Int Meas Confed 128:388–392

23. Qu C-X, Yi T-H, Yang X-M, Li H-N (2017) Spurious mode distinguish by eigensystem realization algorithm with improved stabilization diagram. Struct Eng Mech 63(6):743–750

24. Riveiro B, DeJong MJ, Conde B (2016) Automated processing of large point clouds for structural health monitoring of masonry arch bridges. Autom Constr 72:258–268

25. Schueremans L, Van Genechten B (2009) The use of 3D-laser scanning in assessing the safety of masonry vaults—a case study on the church of Saint-Jacobs. Opt Lasers Eng 47(3–4):329–335

26. Seo HJ (2020) Monitoring of CFA pile test using three dimensional laser scanning and distributed fibre optic sensors. Opt Lasers Eng. https://doi.org/10.1016/j.optlaseng.2020.106089

27. Seo HJ (2021) Long-term Monitoring of zigzag-shaped retaining structure using laser scanning and analysis of influencing factors. Opt Lasers Eng. https://doi.org/10.1016/j.optlaseng.2020.106498

28. Seo HJ (2021) 3D roughness measurement of failure surface in CFA pile samples using three-dimensional laser scanning. Appl Sci. https://doi.org/10.3390/app11062713

29. Seo HJ, Acikgoz S, Zhao Y (2017) Monitoring of retaining wall at tunnel entrance using three dimensional laser scanning. In: The 2017 World Congress on advances in structural engineering and mechanics (ASEM17), Seoul, Korea, 28 Aug.-01 Sep

30. Seo HJ, Choi H, Park J, Park J, Lee IM (2017) Crack detection in pillars using infrared thermographic imaging. Geot Test JASTM 40(3):371–380

31. Seo HJ, Jeong KH, Choi HS, Lee IM (2012) Pullout resistance increase of soil nailing induced by pressurized grouting. J Geotech Geoenviron Eng ASCE 138(5):604–613

32. Seo HJ, Lee IM, Lee SW (2014) Optimization of soil nailing design considering three failure modes. KSCE J Civ Eng 18(2):488–496

33. Seo HJ, Lee IM, Ryu YM, Jung JH (2019) Mechanical behavior of hybrid soil nail-anchor system. KSCE J Civ Eng 23(4):4201–4211

34. Seo HJ, Pelecanos L, Kwon YS, Lee IM (2017) Net load-displacement estimation in soil-nailing pullout tests. Proc Inst Civ Eng Geotech Eng 170(6):534–547

35. Soni A, Robson S, Gleeson B (2015) Structural monitoring for the rail industry using conventional survey, laser scanning and photogrammetry. Appl Geomat 7:123–138

36. Topcon (2012) Instruction manual power station—PS series. Topcon Corporation, Japan

37. Wang W, Zhao W, Huang L, Vimarlund V, Wang Z (2014) Applications of terrestrial laser scanning for tunnels: a review. J Traffic Transport Engg (English Edition) 1(5):325–337

38. Ye C, Acikgoz S, Pendrigh S, Riley E, DeJong MJ (2018) Mapping deformations and inferring movements of masonry arch bridges using point cloud data. Eng Struct 173:530–545

Publisher's Note Springer Nature remains neutral with regard to jurisdictional claims in published maps and institutional affiliations.